Journal of Materials Science and Engineering with Advanced Technology
Volume 2, Number 1, 2010, Pages 41-59

POINT DEFECTS IN AMORPHOUS AND NANOCRYSTALLINE FLUORINATED SILICON FILMS

D. MILOVZOROV

Fluens Technology Group Ltd.
Moscow 107497
Russian Federation
e-mail: dmilovzorov2002@yahoo.com

Abstract

Nanocrystalline fluorinated silicon films are studied by using Raman spectroscopy, electron paramagnetic resonance, Fourier-transformed infrared spectroscopy, atomic force microscopy, nonlinear laser spectroscopy, and photoluminescence. Electrical properties of nanocrystalline silicon and amorphous silicon films were compared. The field-assisted migration of point defects is dramatic for durability and reproducibility properties of devices based on amorphous silicon. The conductivity properties are stable for nanocrystalline silicon film by electric field.

1. Introduction

Polycrystalline and nanocrystalline silicon (nc-Si) are widely used in thin film transistors (TFT), solar cells, and memory devices production. Usually, the TFT characteristics depend on the point defects inside the film or an interface area silicon-silicon dioxide. For pure thin silicon films deposited on glass substrate the point defects [13], such as Pb or dangling bonds, E-centers or even VO (vacancy of oxygen atom in silicon/silicon

Keywords and phrases: nanocrystalline silicon, fluorinated silicon films, point defects, silicon bonds, paramagnetic centers, current-voltage and resistance-voltage characteristics, Raman spectral characteristics.

Received April 30, 2010

dioxide interface) defects, play a great role for electronic structure distortion and changing in optical properties [15]. For silicon films, there are different kinds of point defects included in silicon net. For silicon films prepared by using PECVD of gas mixture silane/silicon tetrafluoride/hydrogen gas mixture, the defects can be detected by electron paramagnetic resonance method [1, 15]. These films were deposited on glass substrates. Also, the impurities' concentrations for oxygen, hydrogen, and fluorine atoms can be easily determined by means of FT-IR spectroscopic technique. The absorption spectral lines can be identified as related to definite silicon bond (Si-O, Si-H or Si-F).

Figure 1 illustrates the three kinds of point defects the quantum properties of which can be switched by applied field. The first is vacancy of the oxygen (VO) defect, the second is E-center with dangling bond of one silicon atom and three silicon atoms with bonds saturated by hydrogen, and the third defect is a defect of fluorine vacancy in silicon fluoride. The oxygen position can be changed by electric or phonon field to switch the $2p_{\mathrm{Si}}3p_{\mathrm{O}}$ orbitals (from p_x to p_z). The applied electric field causes the change of spatial position of charges to change the state by defect migration.

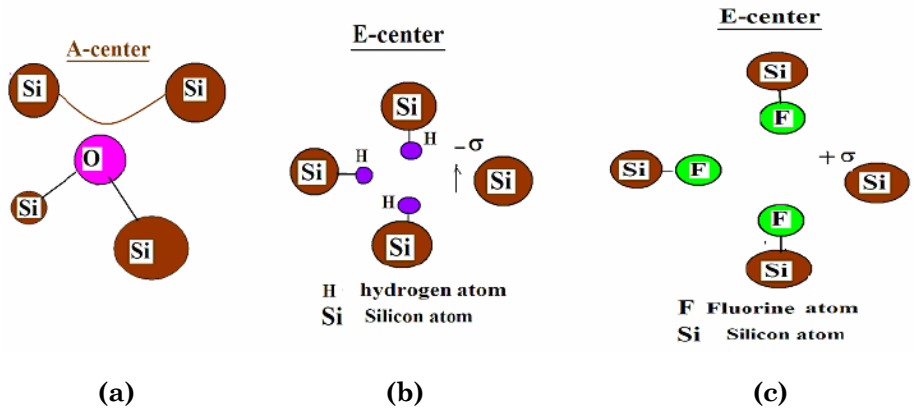

Figure 1. There are three kinds of defects (or paramagnetic centers) in silicon films prepared by using PECVD of gas mixture SiH_4/SiF_4 diluted by hydrogen that can be switched in their states by electrical of phonon field.

2. Experimental Results

The polycrystalline silicon films were prepared by using plasma-enhanced chemical vapour deposition (PECVD) for different silicon structural orders: nanocrystalline and amorphous. Figure 2 illustrates the photo that was made by atomic-force microscope of nanostructured silicon film. The thickness of films was 300nm. The crystalline volume fraction was varied from 0% to 70%. The oxygen concentration in films was varied from 10^{17}cm^{-3} to 10^{21}cm^{-3}. The hydrogen concentration was varied from the value less than 10^{18} to 10^{21}cm^{-3}. Silicon films were fluorinated during their deposition by adding silicon tetrafluoride to the gas mixture of silane diluted by hydrogen.

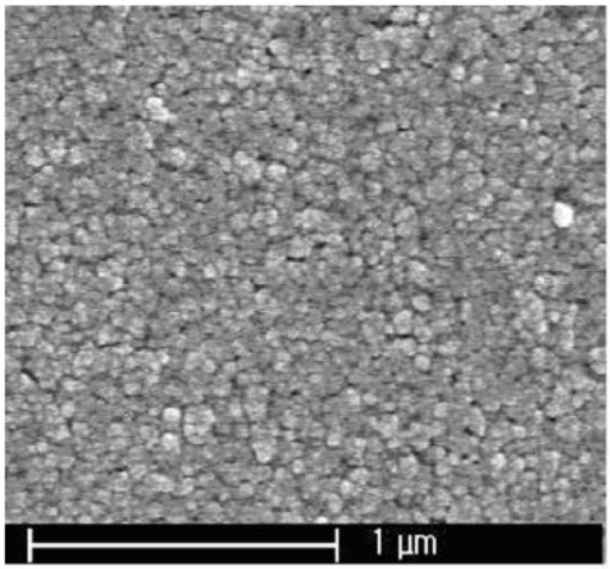

Figure 2. Atomic-force microscope photo of nanocrystalline silicon film.

Raman and photoluminescent (PL) spectra of silicon film are shown on Figure 3. It is seen that the crystalline volume fraction is significant (by estimating the Raman peak around 520cm^{-1}) and luminescent properties are sufficient (in range of photon energy 1.6-1.8eV). It is assumed that the PL response in low energy part is caused carriers

transitions through the defect levels, which values of energies are located near the bottom of conductivity band and top of the valence band. There is a correlation between the density of defects (for example, dangling bonds [11]) and band-tail width value. It is known, also, the Staebler-Wronski effect of defect's generation by light irradiation of silicon film surface [12].

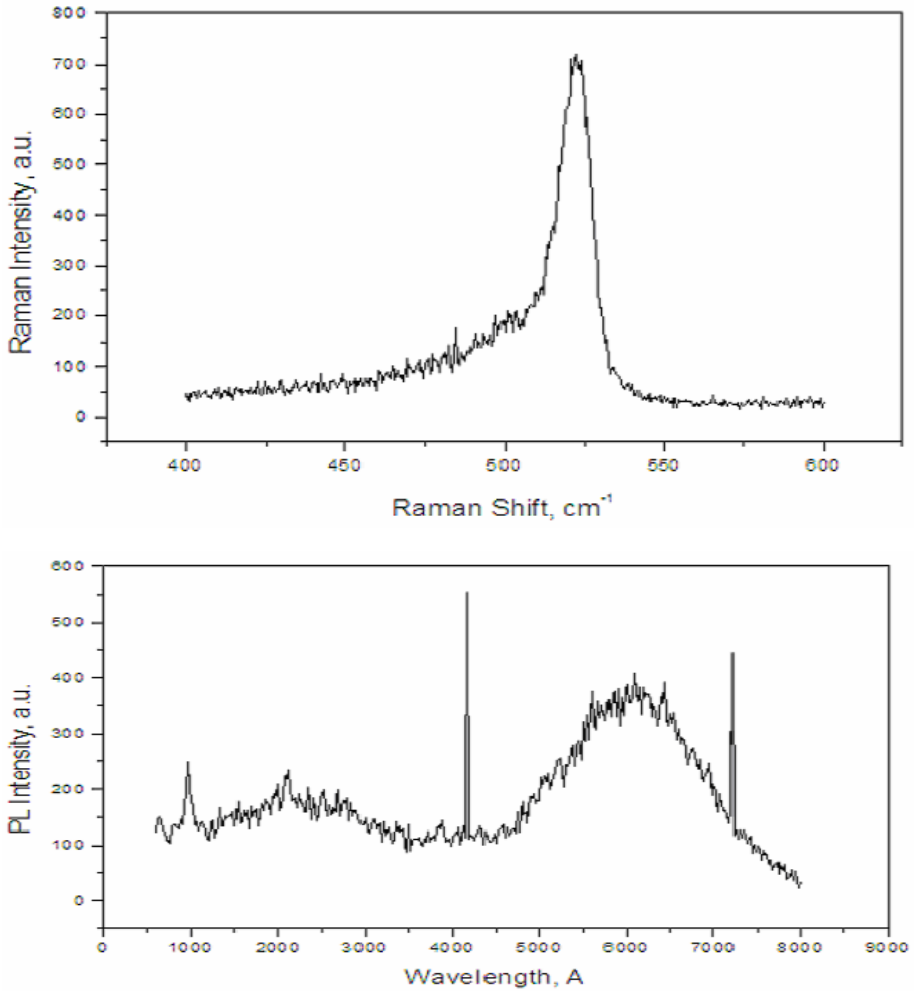

Figure 3. Raman and PL spectra of silicon film with average grain size of nanocrystals 8.3nm (evaluated by means of X-ray diffraction spectrum).

2.1. Oxygen-related defects

Figure 1 (a) illustrates the vacancy of oxygen atom in silicon/silicon dioxide interface and paramagnetic A-center with $3p_{\mathrm{Si}}$- $3p_{\mathrm{Si}}$ [4] molecular orbital (MO) switching by electric field or even phonons. It is seen [6] that, the quantum interference of both two oxygen related levels can be result in $2p_{\mathrm{O}x} \rightarrow 2p_{\mathrm{O}z}$ orbital switching between two silicon atom pairs.

2.2. $\mathbf{Si_3H^{-\sigma}}$ defects

The molecular-like spectrum of electron states for hydrogenated cluster $\mathrm{Si_3H^{-\sigma}}$ has series of electron states in the range from 0.7eV to 1.0eV [17]. The eigen-frequencies of oscillator $\mathrm{Si_3}$-H are conjugated with the electron states for the same oscillators and results in appearance of broadening in electron spectra. The defect illustrated on the Figure 1 (b) can be described as tied three $\mathrm{Si_3}$-H oscillators and one $\mathrm{Si_3}$- oscillator. It is assumed that, the quantum properties of defect are reflected in their molecular orbitals spectral positions. It should be observed surely for nanostructured silicon films with structured cell less than 1nm or for amorphous hydrogenated silicon film. In such kind of media, we can surely change the spectral positions of electron states by using bias voltage.

2.3. $\mathbf{Si_3}$-F related defect

Silicon functional groups can be determined as following Si-Si, F-Si-H, $\mathrm{FSiH_2}$, $\mathrm{SiH_3F_3}$, $\mathrm{SiH_2}$-F. The silicon bonding arranged according to sp^3 hybridization: 3*s* spin-paired electrons and 3*p* electrons. The greatest energy of bonding is for Si-F bond equal to 135kcal/mol, but for Si-H and Si-Si, is 76kcal/mol and 53kcal/mol, respectively. Because, the dipole moments due to the great value of electro-negativity of fluorine atom will be significant. Accordingly, the charge distribution of electron density in $\mathrm{SiH_3}$-F molecular group is following: for Si atom is +1.1, for H atom is –0.15, and for F atom is –0.67 [14]. Figure 4 shows the role of fluorine for weakening of Si-O bonding.

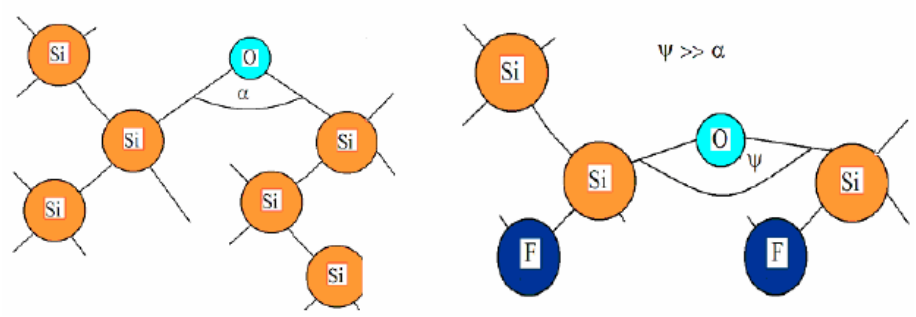

(a) **(b)**

Figure 4. (a) Si-O-Si bonding in silicon film and (b) F-Si-O-Si-F configuration in fluorinated silicon film.

2.4. Symmetry violence in electron density on atomic scale and second-order dipole moments

Figure 5 shows the nonlinear optical spectra for two nanocrystalline silicon films. The signal of second-harmonic generation was detected in the spectral range from 3.2eV to 3.26eV. It is seen that the peak width is around 0.14eV. Usually, the bulk silicon has no second-harmonic response because it is symmetry. But, for thin silicon films with oriented nanocrystals (111), which were deposited on quartz substrates the Si-O dipoles break the symmetry and results in second-harmonic generation. The point defects due to oxygen incorporation in silicon film causes the nonhomogeneity in electron density spatial distribution. The SHG response depends on linear combination of several dipole moments, which contributed into polarization. There are two kinds of dipoles are created by defects such as dangling bonds and oxygen vacancy: dipoles with polarized charges by changes in electron density in silicon atoms, from one side, and dipoles with polarized charges by changes in electron density caused by oxygen great value of electron affinity.

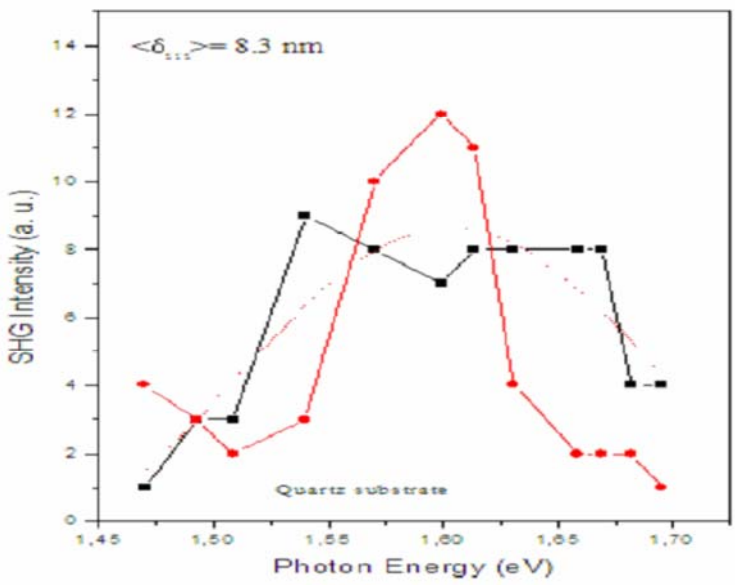

Figure 5. Nonlinear optical spectra for the silicon films with the same average grain size (8.3nm).

The second-order terms of dipole values for polarized media are given by

$$\mu^{(2)} = e\int_0^{V_R}\Psi_{\mathrm{Si}1S}\Psi_{\mathrm{Si}3p}d\nu\Big(\int_0^{V_R}\Psi_{\mathrm{Si}1S}x^2\Psi_{\mathrm{Si}3p}d\nu - \left(\int_0^{V_R}\Psi_{\mathrm{Si}1S}x\Psi_{\mathrm{Si}3p}d\nu\right)^2\Big)\Big/\int_0^{V_R}\Psi_{\mathrm{Si}1S}x\Psi_{\mathrm{Si}3p}d\nu,$$

where V_R is a sphere of integration, x is bond length, we assume that x value is a sum of two covalent radii for both atoms, ξ is a largest covalent radius for two atoms, R is a distance by the atomic orbital for each center has spatial the limit of its extension, for the values of distance $R = 4\xi$, we suppose the averaging procedure is possible. This dipole moment is appeared because of the dangling bonds cause the breaking in crystal

structure's symmetry. The concentration of dangling bonds in silicon film deposited on glass substrate is varied from $10^{16}\,\mathrm{cm}^{-3}$ to $10^{20}\,\mathrm{cm}^{-3}$.

The next two types of dipole moments are caused by the oxygen atom incorporation with silicon and its value can be evaluated as following:

$$\mu^{(2)} = e\int_0^{V_R}\Psi_{\mathrm{Si1}S}\Psi_{\mathrm{O2}p}d\nu\Big(\int_0^{V_R}\Psi_{\mathrm{Si1}S}x^2\Psi_{\mathrm{O2}p}d\nu - \left(\int_0^{V_R}\Psi_{\mathrm{Si1}S}x\Psi_{\mathrm{O2}p}d\nu\right)^2\Big)\Big/\int_0^{V_R}\Psi_{\mathrm{Si1}S}x\Psi_{\mathrm{O2}p}d\nu;$$

$$\mu^{(2)} = e\int_0^{V_R}\Psi_{\mathrm{Si3}p}\Psi_{\mathrm{O2}p}d\nu\Big(\int_0^{V_R}\Psi_{\mathrm{Si3}p}x^2\Psi_{\mathrm{O2}p}d\nu - \left(\int_0^{V_R}\Psi_{\mathrm{Si3}p}x\Psi_{\mathrm{O2}p}d\nu\right)^2\Big)\Big/\int_0^{V_R}\Psi_{\mathrm{Si3}p}x\Psi_{\mathrm{O2}p}d\nu.$$

The first integral in equation describes the charge spatial distribution of two atomic orbital that are located on different centers overlap. The second term in such multiplication in brackets describes the spatial distortion of dipole bond length by various conditions: such as external electromagnetic field or the other coupled Si-O dipole. These changes cause the perturbations in wave-functions, too. However, we estimate such dipole moment distortion by using non perturbative wave-functions and stressed bond with its length more than ordinary. Also, the quadruple moment contributes into SHG response. The point defects, which were shown on Figure 1 can be described as possible model to explain the SHG for silicon films. Classical form for molecular quadruple moment is given by

$$\Theta_{\alpha\beta} = \frac{1}{2}\sum_i e_i(3r_{i\alpha}r_{i\beta} - r_i^2\delta_{\alpha\beta}).$$

The quantum mechanical description of molecular quadruple moment is very complicated. Because, it is possible to use the quantum chemistry results to characterize the optical response of each molecular group. Also, it is clear that, the local molecular surrounding plays a great role in second-harmonic generation from silicon nanocrystalline or amorphous film.

2.5. Absorption spectra for silicon films

Figure 6 shows the spectral peaks related to the oxygen states in silicon film absorption spectrum for molecular oxygen in spectral range from $1000cm^{-1}$ to $1200cm^{-1}$. It is seen that, the Si-F bonds was also, detected in the range from $900cm^{-1}$ to $948cm^{-1}$ (for stretching mode). We suppose that the different molecular SiH_n-F groups contribute into absorption spectral picture. The absorption spectral peaks in the range from $828cm^{-1}$ to $850cm^{-1}$ correspond to the different vibration frequencies of various isotopic oxygen fractions in VO defects and A defects for silicon [1].

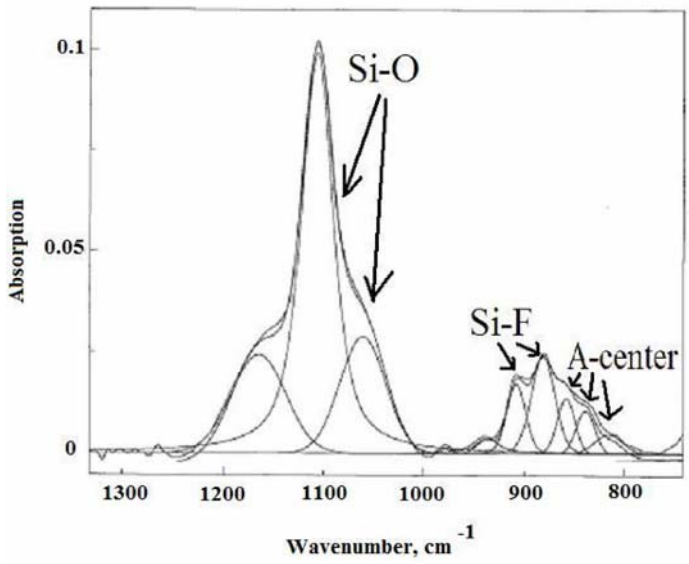

Figure 6. FT-IR spectrum of oxygen- and fluorine-related spectral area for silicon film with grain size 8.3nm.

Quantum properties of point defects are reflected in variations of wavelength of absorption peaks for the oscillators with different eigen-frequencies. The square under the peak is related to the concentration of each bonding. We assume that the fluorine incorporation in silicon film creates new molecular dipoles and changes the existing Si-O dipoles [3], too. Because, the polarization properties for fluorinated glasses and thin silicon films should be strictly depends on fluorine concentration. In addition, the electrical resistance increases by fluorination of silicon film, too. The fluorination results in broadening of band gap for silicon [10].

2.6. EPR experiments

In EPR spectroscopy, the silicon films are irradiated with microwaves with frequency around 9.45GHz and the magnetic field is scanned around the value of resonance energy. Figure 7 shows the EPR spectra: for hydrogenated nanocrystalline silicon (see Figures 7(a) and 7(b)) with crystalline volume fraction more than 70%; the amorphous silicon film (deposited on cerium dioxide buffer layer with thickness 10nm) that contains the 30% of silicon as nanocrystals inserted into amorphous phase; and amorphous silicon film. It is seen that, the content of Pb defects as paramagnetic centers is low for nanocrystalline hydrogenised silicon film and amorphous silicon film with nanocrystals deposited on cerium dioxide buffer layer (see Figure 7(c)), but it is high for amorphous by CVD silicon film (see Figure 7(d)).

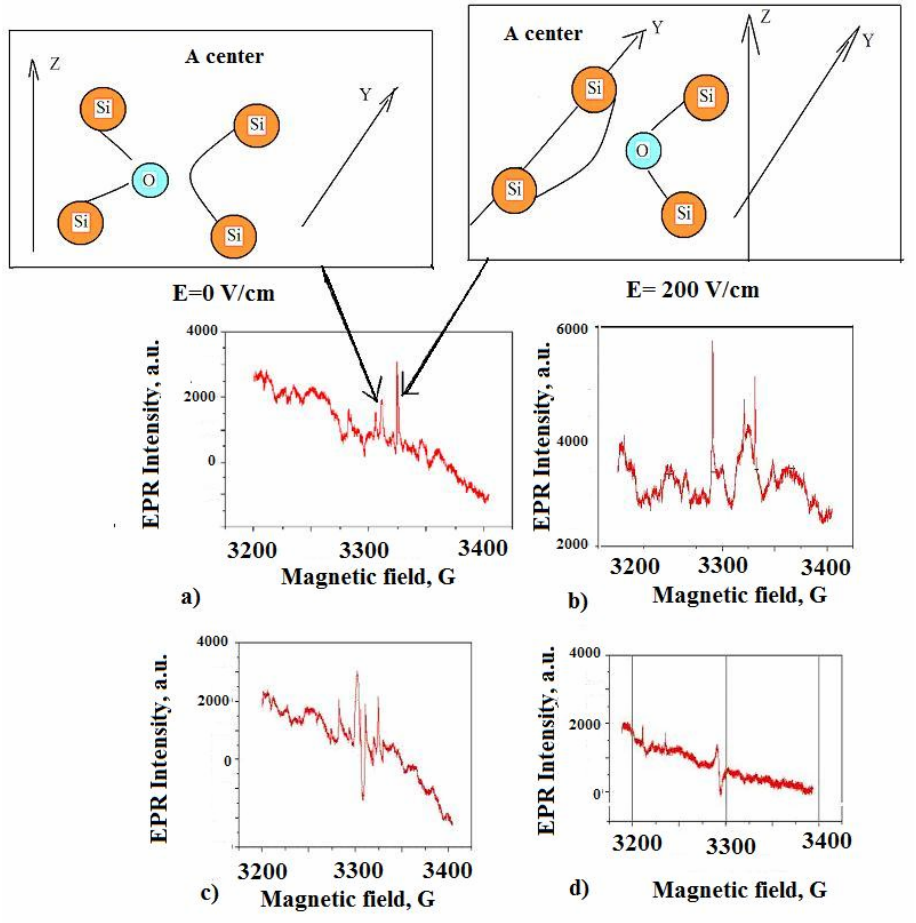

Figure 7. EPR spectral data for nanocrystalline silicon films deposited on glass substrate (a) without applied electric field; (b) by electric field E = 200V/cm; (c) nanocrystalline silicon films deposited on cerium dioxide buffer layer and (d) silicon films partially crystallized by laser beam.

The paramagnetic centers, which named as A-centers were created by two pair of silicon atoms and one oxygen atom results in strong microwave intensity that depends on those configurations. We assume that, the differences in their frequencies are because of variation of oxygen atom incorporation in silicon net and crystal orientation according to the work of Watkins and Corbett [15]. It is supposed that there are two

various frequencies, which were shown in Figure 7(a) correspond to the different oxygen atomic positions in point defect such as A-center. In one sample, the paramagnetic A-centers are partially distributed in their configurations. The fraction values can be estimated as according to the magnitude values evaluation as by using the data of laser time resolved spectroscopy [6]. The applied electric field along the silicon film with value of E = 200V/cm causes the A-centers switching in their magnitudes of signal at oscillation frequencies (see Figure 7(b)). There is a tunnel jumping of oxygen atom in A-center due to the high value of its electron affinity and field-stimulated changes in potential energetic barrier for oxygen atom.

Also, it is necessary to note that, the EPR data, which were shown in Figure 7(c) reflect the increase in EPR magnitude caused by electric field-assisted atom migration for oxygen and cerium atoms from buffer layer in silicon film. Such atomic electron migration results in E-center's creation into thin silicon film. The silicon crystal phase destruction due to the electric field effect [5] from one side and the appearance of polarized charges in Si-O bonding, from another side, are possible mainly due to the migration of oxygen atoms. The concentration of dangling bonds increases, too. The magnitude of EPR intensity is higher than that for a-Si sample as it is seen from Figure 7(d). It is assumed that, such increasing in EPR magnitude is caused the resonance effects not only due to the paramagnetic centers inside the silicon film, but because of cerium dioxide with the same bond legnth of Ce-O configuration that results in appearance additional paramagnetic centers.

2.7. Field effect in Raman spectra for amorphous and nc-Si films

The experimental investigations by Raman scattering spectroscopy of silicon films were carried on by means of spectroscopic technique JASCO NRS-1000 (Japan). Figure 8 shows the electrical field stimulated changes in Raman spectral characteristics for amorphous (see Figures 8(a) and (c)) and nanocrystalline silicon films (see Figures 8(b) and (d)). It is seen, that external applied electric field along the surface of substrate does not change the spectral characteristics.

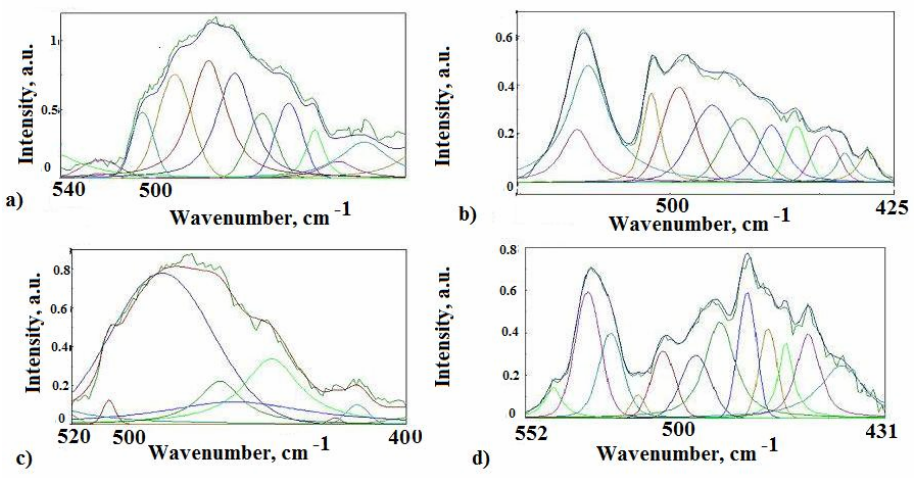

Figure 8. Raman spectra from amorphous (a) and nanocrystalline (b) silicon thin films deposited by PECVD (with thickness less than 100nm); by applied external lateral electric field 3.0 10^6 V/cm from amorphous (c) and nanocrystalline (d) silicon thin films.

The electric field value was 3 μV/Å. It is assumed that, the changes of spectral characteristics reflect the chemical bonding changes by electric field-assisted migration effect. The diffusion coefficient for point defect such as dangling bond or impurity as hydrogen atom is given by:

$$D = D_0 \exp\left(-\frac{Q_A}{kT}\right),$$

where Q_A is activation energy. The a-Si film consists of high fraction of weak bonding of silicon because of oxygen or hydrogen incorporation into silicon. The homogeneity in chemical bonding properties of amorphous silicon film increases by applied external electric field mainly due to the Si-O dipole reorientation, migration of dangling bonds, and hydrogen atoms. However, for nc-Si film, we can observe the strictly different tendency in structural order changes. It is seen that for nc-Si film, the sharp spectral peaks in Raman spectra are appeared, but for amorphous silicon bonding, there is a smooth broad peak. The oxygen incorporation

with silicon nanocrystals with dominant orientation (111) changes the Si-Si bonds and phonon energetic diagram. The point defects can migrate only in grain boundary region. By applied electric field, all the oxygen atoms migrate inside the film and cause the anisotropic deformation in silicon bonds. The orientation of all Si-O dipoles is changed by this way to compensate the external electric field. There are two structural order tendencies: the orientation of bonds along the applied external electric field, from one side, and the bonding according to the structural order of silicon for crystal orientation (111). Such kind of structural anisotropy reflects in sharp increasing the densities of silicon bonds. We assume that the production of silicon films with determined spatial anisotropy is possible.

2.8. Electrical measurements

Figure 9 illustrates the current-voltage and resistance-voltage characteristics for nanocrystalline and amorphous silicon films. It is seen that the resistance for nanocrystalline films are independent of voltage variations, but for amorphous film, there is an unstable behavior of resistance value. The Si-O dipoles are reoriented by external electric field. Because, there is a hydrogen and point defect's migration such as dangling bonds. For nanocrystalline fluorinated films, there is no oxygen inside the film. The electrical resistance is determined by existence of Si-F bonds, which are fixed in their spatial positions in film.

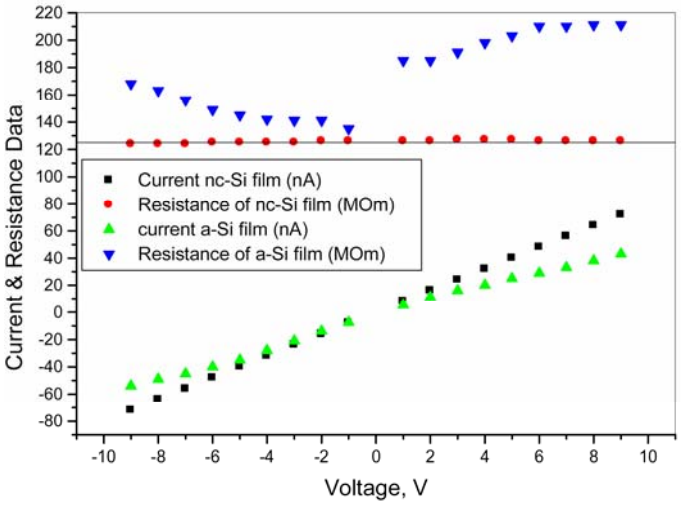

Figure 9. Current-voltage and resistance-voltage characteristics for nanocrystalline and amorphous silicon films.

3. Discussion

We investigated the role of oxygen-related defects in optical properties of silicon film. The Si-O bonding generates defects inside film that differ each from other by variations in hydrogen termination degree. Quantum properties depend on the molecular orbitals of Si-O bond. The molecular orbitals can be meta-stable for the different oxygen incorporation into silicon film [15]. We studied the role of defects in silicon film and their quantum properties reflected in optical responses.

3.1. Quantum tunneling model for oxygen atom in silicon

The electric field applied to the nanostructured silicon thin film gives the new possibility to change structural order. Such kind of structural transformation is caused because of there are numerous defects inside the silicon film. The oxygen atoms and dimers are incorporated in the silicon grain boundary and have weak covalent bonds with silicon. But, the activation energy for molecular diffusion is low, 0.3eV, in contrast with the activation energy value for atomic diffusion (1.3eV). The energy of Si-O-Si bridge interaction (see Figure 10) can be written in the form of Morse function

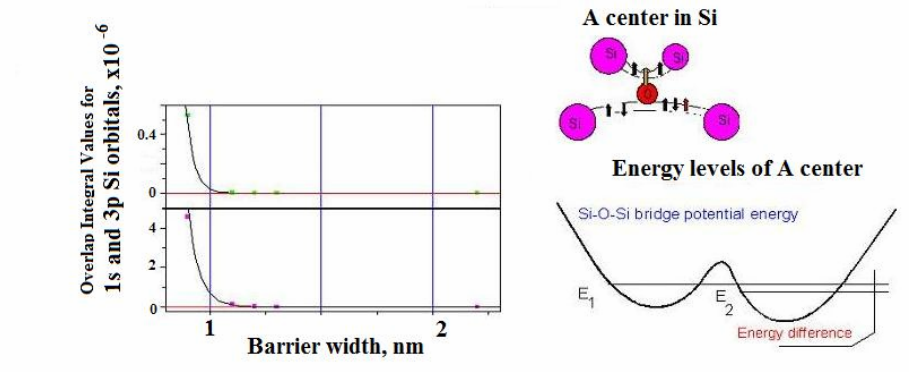

Figure 10. Overlapping integrals for Si and O atoms incorporated into Si-O bond (a), potential energy as a function of an oxygen atomic position from the two silicon atom pairs, there is an energy difference in oxygen atom spectra because of the orbitals switching from p_x to p_z.

$$U = U_0(1 - \exp(-\alpha(x - d)))^2 + U_0(1 - \exp(-\alpha(x + d)))^2,$$

where U_0 is the energy of $\mathrm{Si\text{-}O}(4.5\mathrm{eV})$, α is coefficient. The oxygen atom in A-center oscillates between two points of stable positions. Transition of probability for oxygen atom through the potential barrier by applied external electrical field $U(r) = U_0 - Er$ is given by

$$T = \nu \exp\left(-\frac{2}{\hbar}\right)\int_{r_1}^{r_2} dr\sqrt{2M(U(r) - E_l)},$$

where ν is a frequency of oscillations of oxygen atom. Wave-function of the oxygen atom is following:

$$\Psi = a_1|\varphi_1> \exp\left(-i\frac{E_1}{\hbar}t\right)\exp(-\Gamma_1 t) + a_2|\varphi_2> \exp\left(-i\frac{E_2}{\hbar}t\right)\exp(-\Gamma_2 t),$$

where φ_1 and φ_2 are the wave functions of pure states 1 and 2, Γ_1 and Γ_2 are the widths of the levels, respectively. We assume that all the Γ values are approximately equal to each other. Raman scattering data help to determine the dipole Si-Si orientation along the laser E-field axe of

incident radiation on the silicon surface by applied electric field switching of O atom spatial position. Applied electric field causes the tunnel of oxygen atom from one pair of coupled silicon atoms to another with perpendicular axis of dipole orientation (see Figure 10). The annealing procedure can assist to restore spectral characteristics related to the primary ordered atomic position due to the minimums in potential energy diagrams. According to the di-interstitial model [5], by the temperature 300°C only di-interstitial reorientation can be observed. Also, for E-defect centers, the annealing to temperature 200°C can cause the defect reorientation, too. Also, the using of electrical field-stimulated to switch the eigen-frequencies of A-center can be surely applied to produce new memory device with diameter of one unit near 1nm [8] or quantum computing element [7].

3.2. Possible mechanisms of defect reorientation

To investigate the role of applied electric field in order-disorder transition, we will propose several mechanisms of electric dipoles creation. The first is the silicon-oxygen (Si-O) or silicon fluorine (Si-F) bonding changes and reorientation of VO or VF defects. These bonding are strongest for silicon film, due to the high electron affinities values for O and F atoms. The dipoles Si-O, Ce-O, and Si-F have the great values in their polarized charges. Because, the interaction between them and electromagnetic field is sufficient that results in their efficient reorientation in amorphous phase of silicon.

The second mechanism of order-disorder transition in silicon film was initially proposed by Watkins and Corbett [16], which is devoted to hydrogen atom reorientation around the vacancy by the temperature above 200°C as possible EPR data explanation. For nanostructured silicon thin film that contains the great amount of tiniest nanocrystals, the hydrogen atoms are distributed in grain boundary of nanocrystal silicon grains. But, by electric field application to the thin film along the surface, the smallest nanocrystals are disappeared and, partially, the crystal structure was destroyed. By annealing, the opposite tendency is

observed. The third assumption is the creation of excited hydrogen molecule inside the silicon film by annealing to the temperatures $150-200°C$: $Si-H + Si-H \rightarrow Si-Si + H^*_2$ [2]. It is clear that the silicon nanocrystals volume fraction decreases, but content of amorphous phase significant increases.

4. Conclusion

Point defects are observed by using various spectroscopy methods. It is observed the field assisted switching of optical properties of silicon films. The role of impurities such as oxygen and fluorine is significant to control the stability of film in its conductivity properties. We confirm that, the successful manufacturing the electronic devices based on nanocrystalline silicon film with great performance particularly, electric field stability, light irradiation, and thermal stability, is more realistic than that, which is done by using amorphous silicon.

Acknowledgement

D. Milovzorov thanks the researches and professors of Physical Department of Moscow State University for useful discussions and help in EPR experiments.

References

[1] J. W. Corbett, G. D. Watkins, R. M. Chrenko and R. S. McDonald, Phys. Rev. 121 (1961), 1015.

[2] B. Jones, B. J. Coomer, J. P. Goss, B. Hourahine and A. Recende, In special defects in semiconductor materials edited by R. P. Agarwal.

[3] Y. Kim, M. Hwang, H. Kim, J. Kim and Y. Lee, J. Appl. Phys. 90 (2001), 3367.

[4] M. Lanoo and G. Alan, Solid State Comm. 28 (1978), 733.

[5] M. E. Law, Y. M. Haddara and K. S. Jones, J. Appl. Phys. 84 (1998), 3555.

[6] D. Milovzorov, Electrochemical and Solid State Letters 4(7) (2001), 61-63.

[7] D. Milovzorov, Quantum logical elements for computing based on polycrystalline silicon, Proceedings of SPIE Photonics and Nanostructures 5361 (2004), 108-116.

[8] D. Milovzorov, Memory cell with photoacoustic switching, Proceedings of SPIE 5592 (2005), 427-437.

[9] D. Milovzorov, Field-effect on crystal phase of silicon in $Si/CeO_2/SiO_2$ structure, Journal of Nanomaterials, Volume 2008, Article ID 712985, 4 pages, 2008.

[10] L. Pan, Y. Ee, C. Sun, G. Yu, Q. Zhang and B. Tay, J. Vac. Sci. Technol. B 22(2) (2004), 583.

[11] Z. Smith and S. Wagner, Phys. Rev. Lett. 59 (1987), 688.

[12] D. Staebler and C. Wronski, J. Appl. Phys. 51 (1980), 3262.

[13] K. Tanaka, E. Maruyama, T. Shimada, H. Okamoto and T. Sato, Amorphous Silicon p.79, John Wiley & Sons, Chichester, 1999.

[14] M. Voronkov, Top. Current. Chem. 131 (1986), 99.

[15] G. D. Watkins and J. W. Corbett, Phys. Rev. 121 (1961), 1001.

[16] G. D. Watkins and J. W. Corbett, Phys. Rev. A138, (1965), 543.

[17] C. Xu, T. Taylor, G. Burton and D. Neumark, J. Chem. Phys. 108 (1998), 7645.

■